Phase-Only Synthesis of a Reflecting Surface for Enhancing Coverages in Urban Scenarios

(Article begins on next page)

Phase-Only Synthesis of a Reflecting Surface for Enhancing Coverages in Urban Scenarios

S. Ayaz(1), M. Beccaria(1), A. Capozzoli(2), C. Curcio(2), G. D'Ambrosio(2), A. Freni(3), A. Liseno(2), and P. Pirinoli(1)

(1) Politecnico di Torino, Dipartimento di Elettronica e Telecomunicazioni, Torino (Italia) (e-mail: paola.pirinoli@polito.it)
(2) Università di Napoli Federico II, Dipartimento di Ingegneria Elettrica e delle Tecnologie dell'Informazione, Napoli (Italia) (e-mail: a.capozzoli@unina.it)
(3) Università di Firenze, Dipartimento di Ingegneria dell'Informazione, Firenze (Italia) (e-mail: angelo.freni@unifi.it)

***Abstract*—A Phase-Only power pattern synthesis of a flat reflecting surface is presented to scatter a beam with a flat-top shaped pattern in one cut and a cosecant pattern in the other one. Far-field illumination is assumed and the reflecting surface is appointed to reflect the impinging wave into a non-specular direction. Also by comparisons with CST studio suite simulations, the results show how, in a realistic urban scenario, the algorithm is capable to effectively enforce the design specifications.**

***Index Terms*—Reflecting surfaces, shaped-beam antennas, Phase-Only synthesis.**

I. Introduction

In recent years, attention has been devoted to improving the performance of wireless communication channels in terms of high channel capacity, high data rates, and coverage capabilities.

To this end, reflecting surfaces have been proposed to establish alternative communication channels whenever transmitters and receivers are not in the line-of-sight [1]–[3]. Indeed, a reflecting surface is able to properly scatter an impinging electromagnetic wave providing it with desired features such as beam shaping, simultaneous multiple beams or beam scanning. Modern scattering surfaces have to be also able to dynamically change their electromagnetic characteristics.

Two main approaches are employed to implement a scattering structure [1].

The first one is based on reflecting arrays. In this case, the reflecting surface is made of elements with sizes and spacings comparable to half a wavelength. In the second approach, metasurfaces made by meta-atoms with sub-wavelength dimensions and spacings are exploited [1].

The attention has been mainly focused, up to now, on controlling the beam pointing direction with weak design specifications on the Side Lobe Level (SLL), the beamwidth, or the beam shape [5], [6]. Thus, the synthesis techniques typically employed in such a framework do not fully exploit all the available degrees of freedom of the structure.

More sophisticated synthesis algorithms to design structures with improved features have been proposed in [4], [7]–[9]. Nevertheless, to successfully design a structure by correctly predicting its behavior, a synthesis approach should be based on an accurate scattering model describing the structure and exploiting a global optimization procedure capable of skipping sub-optimal solutions. Unfortunately, accurate models to be employed in global optimizations involve a very high computational complexity as discussed in [10]–[12]. Accordingly, design procedures to reduce computational burden and to keep at the same time high performance are needed.

Typically, a multi-stage approach can be employed to trade off accuracy and computational complexity [10]–[12]. Throughout the different stages, the number of unknowns is progressively increased by exploiting proper modal representations. In particular, at the first stages, an approximate model with few unknowns is considered. In the subsequent stages, the accuracy of the models is progressively increased, by also using less computationally burdensome optimization techniques. Here, we consider the use of Phase-Only synthesis, often adopted at the initial stages of the procedure, to design a reflecting surface for enhancing coverages in urban scenarios.

In this work, a scattering structure with elements that have dimensions and spacings close to half wavelength has been considered. Furthermore, the results of the first Phase-Only step of the mentioned multistage technique have been reported [11].

II. Phase-Only Model

We assume a flat periodic reflecting surface arranged on an NxM Cartesian grid, with spacings p_x and p_y along the x-axis and y-axis, respectively, and located on the $z = 0$ plane, see Fig. 1. The reflecting surface is assumed to be illuminated by a plane wave [4], [6], even if the proposed synthesis approach can also be extended to the case of different illuminations.

Accordingly, the electric field impinging on the element $(n\ m)$ is assumed to be:

$$\underline{E}_{f_{nm}} = \underline{E}_{0_i} e^{-j(u_i x_{nm} + v_i y_{nm})} \tag{1}$$

where $u_i = \beta sin(\theta_i)cos(\phi_i)$, $v_i = \beta sin(\theta_i)sin(\phi_i)$, (θ_i, ϕ_i) are the angles of incidence of the locally impinging plane wave, $\beta = \frac{2\pi}{\lambda}$, λ being the wavelength and (x_{nm}, y_{nm}) the reflecting element positions.

The scattering features of element $(n\ \ m)$ are modeled by considering a scattering matrix $\underline{\underline{S}}_{nm}(u, v)$, where $u = \beta sin(\theta)cos(\phi)$, $v = \beta sin(\theta)sin(\phi)$ and (θ, ϕ) are the observation directions. The dependence of $\underline{\underline{S}}_{nm}(u, v)$ from the impinging direction is skipped since the impinging direction is the same for all the elements. The scattering matrix is appointed to return the (θ, ϕ) components of the reflected field once the (θ, ϕ) components of the impinging field are given.

According to the Phase-Only model, the scattering matrix of each element is modeled as

$$\underline{\underline{S}}_{nm}(u,v) = \underline{\underline{S}}_0(u,v)e^{j\psi_{nm}}, \tag{2}$$

where the term $\underline{\underline{S}}_0(u,v)$ is common to all elements, each element introduces a phase shift ψ_{nm} to the incident field and the dependence of $\underline{\underline{S}}_0(u,v)$ from the impinging direction has been omitted.

The far-field pattern of the scattered field based on the Phase-Only model can be thus written as [10], [11]:

$$\begin{pmatrix} F_{co} \\ F_{cr} \end{pmatrix}(u,v) = \underline{\underline{Q}}(u,v)\underline{\underline{S}}_0(u,v)$$

$$\sum_{n=0}^{N-1}\sum_{m=0}^{M-1} \underline{E}_{f_{nm}} e^{j\psi_{nm}} e^{j(ux_{nm}+vy_{nm})}, \tag{3}$$

where F_{co} and F_{cr} are the co-polar and cross-polar components of the scattered far-field pattern and $\underline{\underline{Q}}(u,v)$ is the matrix converting the (θ,ϕ) components to the corresponding co-polar and cross-polar ones.

III. Synthesis Strategy

A synthesis based on the Phase-Only model typically controls only the co-polar pattern. The design specifications are so enforced by mask functions (m_{co}, M_{co}) providing lower and upper bounds, respectively, to the admissible power pattern of the co-polar component only [10]–[12].

The aim of the Phase-Only synthesis is to evaluate the unknown phase shifts minimizing a cost functional Φ describing the distance between the far-field power pattern and its projection on the set u_{co} of admissible power patterns.

$$\Phi(\underline{\psi}) = \| \, |F_{co}|^2 - Pu_{co}(|F_{co}|^2) \|^2 \tag{4}$$

where $\|.\|$ is the L^2 norm and $Pu_{co}(\cdot)$ is the projection operator over the set u_{co}. Herein, the generalized projections technique has been employed to minimize Φ [11].

The Phase-Only stage is also divided into two steps to initially restrain the number of unknowns and then increase them [10], [11].

In the first step, the unknown phases are expanded by using few Zernike polynomials.

$$\psi_{nm} = \sum_{t=1}^{T} c_t Z_t(x_{nm}, y_{nm}) \tag{5}$$

where the Z_t's are the Zernike polynomials up to the T-th order.

In the second step, the unknown phases have been represented by means of pulse basis functions to effectively exploit all the degrees of freedom offered by the Phase-Only model.

Moreover, the gradient of the cost functional Φ has been evaluated analytically to limit the computational burden and to improve the synthesis performance [11].

IV. Design Specifications

The design specifications have been enforced by considering the scenario depicted in Fig. 2. A base station is considered as the source of the primary field. The region to be covered by the scattered field is that highlighted in orange in Fig. 2 representing a street assumed shadowed with respect to the primary field. A reflecting surface is introduced to improve the street coverage.

The beam is assumed flat-top in the horizontal plane (u-cut) and with a cosecant shape in the vertical one (v-cut).

The flat-top beam is useful to cover the entire width of the street. On the other hand, the cosecant beam is exploited to compensate for the different distances of the reflecting surface to all the points along the street and so to achieve uniform illumination.

For the case of study, the angle, under which the street is illuminated, is assumed equal to $\Delta\Theta = 6.5^o$ (green curve in Fig. 2), while $(\theta_i, \phi_i) = (20^o, 0^o)$ are the angles of incidence of the impinging plane wave. Furthermore, the beam is tilted in the xz plane to point to the $(\theta,\phi) = (30^o, 180^o)$ direction, different from the specular one.

The mask functions have been defined to enforce a $SLL = -22$ dB.

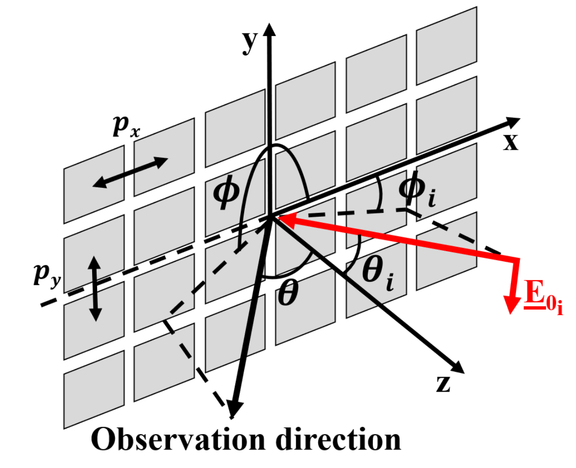

Fig. 1. Problem Geometry.

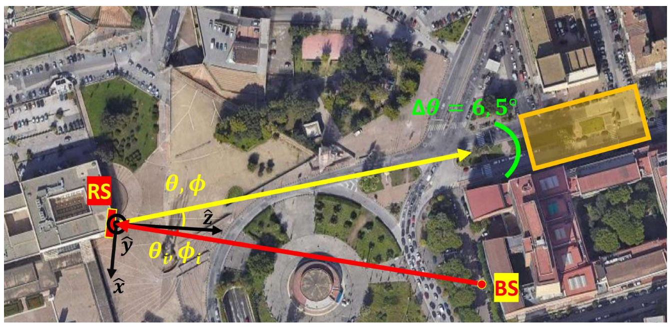

Fig. 2. The urban scenario of interest.

V. UNIT-CELL

The reflecting surface has been realized using resonant elements with a size comparable to half wavelength. A square unit-cell with side $p_x = p_y = 5.45\ mm$ has been considered. The metallic patch of the unit-cell is a square of side W and it is printed on a grounded dielectric DiClad527 substrate ($\epsilon_r = 2.55$, $tan\delta = 0.0022$ and thickness $h = 0.8\ mm$) [4], [13]. The scattering matrix $\underline{\underline{S}}_0(u, v)$ and the behavior of the phase of the reflection coefficient in Fig. 3 have been evaluated using Altair FEKO according to a Floquet modelling.

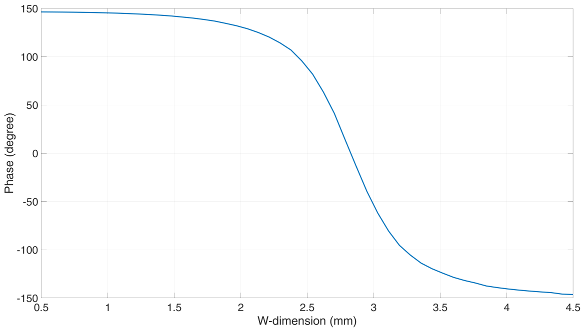

Fig. 3. The phase of the reflection coefficient with incident plane wave angle $(\theta_i, \phi_i) = (20^o, 0^o)$, at $f_0 = 27$ GHz.

VI. RESULTS

An operating frequency of $f_0 = 27$ GHz has been considered and a reflecting surface composed of $N = 35$ elements along the x-axis and $M = 64$ elements along the y-axis has been dealt with.

The synthesis specifications are illustrated by Figs. 4 and 5 referring to the u- and v-cut, respectively. Nevertheless, in order to adequately deal with the issue of the specular reflection contribution, of a non-full efficiency of some of the reflecting elements and of model errors, proper mask functions have been considered during the synthesis process (see Fig. 6 for the u-cuts).

The optimization performed by the Phase-Only synthesis returns the directivity pattern in Fig. 7, wherein also the mask function footprints are reported as black lines. On the other hand, u- and v-cuts of the synthesized and normalized far-field pattern are reported in Figs. 8 and 9 (red lines), respectively, along the directions indicated in red in Fig. 7. As can be seen, the synthesized far-field pattern satisfactorily meets the design specifications. The whole structure has been simulated in the CST studio suite to test the validity of the synthesis strategy. Before CST simulation, the accuracy of the model has been increased to refine the predicted solution. The simulated cuts in Figs. 8 and 9 (blue lines) are in good agreement with the synthesized ones. In the u-cut, the side-lobes close to the main beam exceed the upper mask, but they are in any case below $-18dB$.

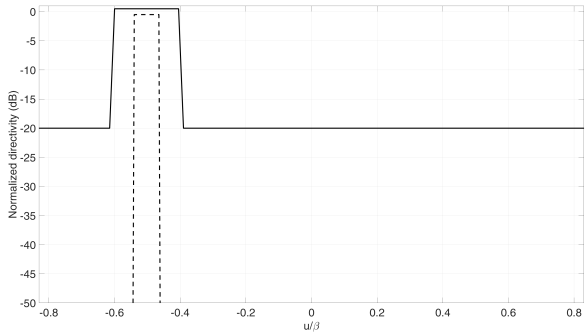

Fig. 4. Specifications: u-cut

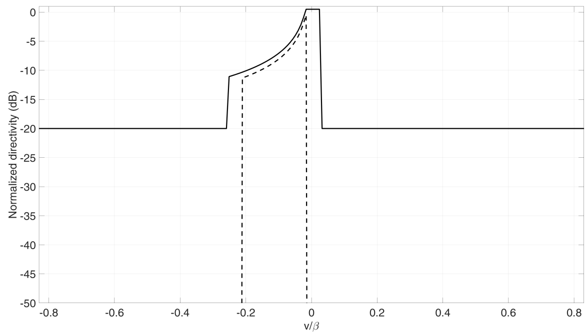

Fig. 5. Specifications: v-cut

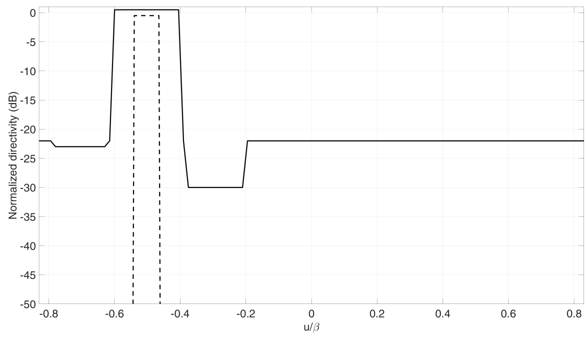

Fig. 6. u-cuts of the mask functions employed during the synthesis.

VII. CONCLUSIONS

A Phase-Only power pattern synthesis to enhance coverages in urban scenarios has been presented and applied to the design of a flat reflecting surface scattering a beam with a flat-top shaped pattern in one cut and a cosecant pattern in the other one. Future developments concern the full multi-stage algorithm using an accurate electromagnetic model to take into account all the degrees of freedom of the reflecting surface and to improve the performance of the achieved far-field pattern.

ACKNOWLEDGEMENT

This work was partially supported by the European Union under the Italian National Recovery and Resilience Plan (NRRP) of NextGenerationEU, partnership on “Telecommunications of the Future” (PE00000001 - program “RESTART”)

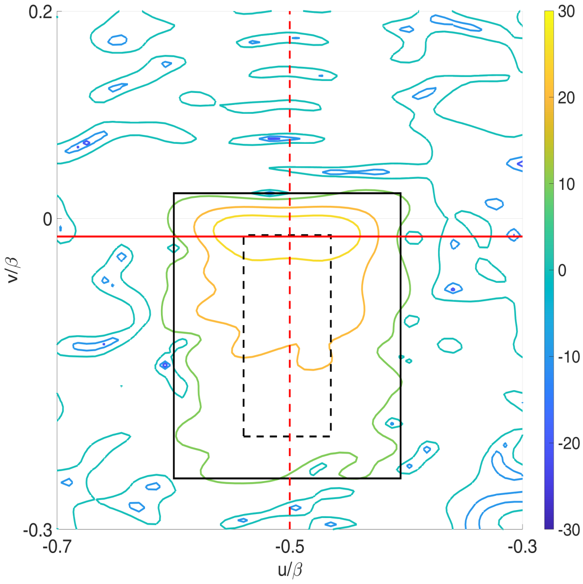

Fig. 7. Synthesized directivity pattern in the (u, v) plane, along with the mask function footprints (black lines; dashed: lower; solid: upper).

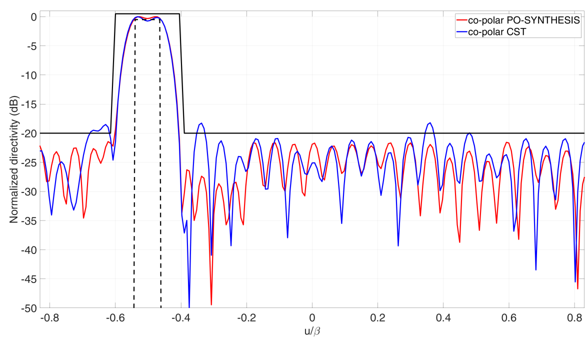

Fig. 8. Red solid line: synthesized and normalized u-cut of the far-field pattern - Blue solid line: simulated u-cut of the far-field pattern in CST - black dashed line: lower mask - black solid line: upper mask.

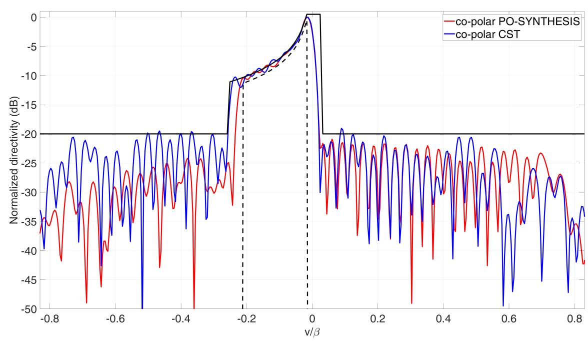

Fig. 9. Red solid line: synthesized and normalized v-cut of the far-field pattern - Blue solid line: simulated v-cut of the far-field pattern in CST - black dashed line: lower mask - black solid line: upper mask.

References

[1] M. A. ElMossallamy, H. Zhang, L. Song, K. G. Seddik, Z. Han and G. Ye Li, "Reconfigurable Intelligent Surfaces for Wireless Communications: Principles, Challenges, and Opportunities", *IEEE Trans. Cogn. Commun. Netw.*, vol. 6, no. 3, Sept. 2020, pp. 990-1002.

[2] Y. Liu, X. Liu, X. Mu, T. Hou, J. Xu, M. Di Renzo and N. Al-Dhahir, "Reconfigurable Intelligent Surfaces: Principles and Opportunities", *IEEE Commun. Surv. Tutor.*, vol. 23, no. 3, 2021, pp. 1546-1577.

[3] E. Basar, M. Di Renzo, J. De Rosny, M. Debbah, M. S. Alouini and R. Zhang, "Wireless Communications Through Reconfigurable Intelligent Surfaces", *IEEE Access*, vol. 7, Sept. 3, 2019, pp. 116753-116773.

[4] A. Freni, M. Beccaria, A. Mazzinghi, A. Massaccesi, P. Pirinoli, "Low-Profile and Low-Visual Impact Smart Electromagnetic Curved Passive Skins for Enhancing Connectivity in Urban Scenarios," *Electronics*, vol. 12, no. 21, p. 4491, Nov. 2023.

[5] T. J. Cui, M. Q. Qi, X. Wan, J. Zhao and Q. Cheng, "Coding metamaterials, digital metamaterials and programmable metamaterials", *Light Sci. Appl.*, 2014, pp. 1-9.

[6] J. B. Gros, V. Popov, M. A. Odit, V. Lenets, and G. Lerosey, "A Reconfigurable Intelligent Surface at mmWave Based on a Binary Phase Tunable Metasurface", *IEEE open j. Commun. Soc.*, vol. 2, May 2021, pp. 1055-1064.

[7] A. Bagheri, M. Safaei, A. Araghi 1, S. M. M. Shahabi, F. Wang, M. Khalily and R. Tafazolli, "Mathematical Model and Real-World Demonstration of Multi-Beam and Wide-Beam Reconfigurable Intelligent Surface", *IEEE Access*, vol. 11, Mar. 2023, pp. 19613-19621.

[8] Y. Wang, C. Pang, Q. Wang, Y. Mu, Y. Cheng and J. Qi, "Phase-Only Compact Radiation-Type Metasurfaces for Customized Far-Field Manipulation", IEEE Trans. Microw. Theory Techn., vol. 71, no. 9, Sept. 2023, pp. 4119-4128.

[9] X. Meng, M. Nekovee and D. Wu, "The Design and Analysis of Electronically Reconfigurable Liquid Crystal-Based Reflectarray Metasurface for 6G Beamforming, Beamsteering, and Beamsplitting", *IEEE Trans. Microw. Theory Techn.*, vol. 9, Nov. 2021, pp. 155564-155575.

[10] A. Capozzoli, C. Curcio, A. Liseno and G. Toso, "Phase-Only Synthesis of Flat Aperiodic Reflectarrays", *Prog. Electromagn. Res.*, vol. 133, 2013, pp. 53-89.

[11] A. Capozzoli, C. Curcio, A. Liseno and G. Toso, "Fast, Phase-Only Synthesis of Aperiodic Reflectarrays Using NUFFTs and CUDA", *Prog. Electromagn. Res.*, vol. 156, 2016, pp. 83-103.

[12] A. Capozzoli, C. Curcio and A. Liseno, "Fast power-pattern synthesis of 2D, planar, aperiodic arrays" in *Int. Conf. on Electromagn. in Adv. Apps*, pp. 746-748.

[13] M. Beccaria, A. Freni, A. Mazzinghi, A. Massaccesi and P. Pirinoli, "Curved Electromagnetic Skins for Urban Scenarios," *2024 18th European Conference on Antennas and Propagation (EuCAP)*, Glasgow, United Kingdom, 2024, pp. 1-5.